Fame, M.L., Spotila, J.A., Owen, L.A., Dortch, J.M., and Shuster, D.L., 2018, Spatially heterogeneous post-Caledonian burial and exhumation across the Scottish Highlands: Lithosphere, https://doi.org/10.1130/L678.1.

GSA Data Repository Item 2018139

Supplementary Material

SUPPLEMENT 1. AHe AND AFT AGES FROM PRIOR WORK ACROSS THE SCOTTISH HIGHLANDS

Figure DR1. The map area is from inset II in Figure 2 and all ages are in millions of years (Ma). AFTA ages, in boxes without outlines, from previous studies are represented by white squares (Thomson et al., 1999), black squares (Holford et al., 2009) and white diamonds (Jolivet, 2007). Grey squares show the sample locations and AFTA ages, in boxes without outlines, and AHe ages, in boxes with black outlines, from Sgorr Dhonuill (SD) (Persano et al., 2007). White circles show sample locations from this study with AHe ages in larger font then summarized prior work.

SUPPLEMENT 2. AGE VERSUS eU FOR ALL AGE DETERMINATIONS

Figure DR2: Each graph displays age versus eU (effective Uranium) for all individual age determinations for all aliquots of each apatite sample analyzed. Grey points show age determinations that were used in calculation of the mean AHe age and white diamonds represent age determinations deemed anomalous (see text for discussion) and were culled prior to the calculation of mean AHe age (Table 1).

SUPPLEMENT 3. QTQT FORWARD MODEL INPUT PARAMETERS

Table DR1. Qtqt forward model (figure 4) input parameters

SUPPLEMENT 4. APATITE ^{4}HE/^{3}HE THEMOCHRONOMETRY

^{4}He/^{3}He Methods

Apatite ^{4}He/^{3}He thermochronometry more tightly constrains the t-T path of an individual apatite as it cooled through the PRZ than does its bulk AHe age alone (Shuster and Farley, 2005, 2004). We analyzed four low-elevation samples using ^{4}He/^{3}He thermochronometry, samples ScT1 from Invershiel, ScT2 from Cluanie, and samples ScT10 and ScT11 from Glen Nevis to better define the most recent cooling histories. We conducted ^{4}He/^{3}He thermochronometry at the Noble Gas Thermochronometry Lab of the Berkley Geochronology Center following analytical methods detailed in Tremblay et al. (2015). After irradiation with 220 MeV protons, we selected single, euhedral crystals for analysis (Shuster and Farley, 2005). We then sequentially degassed the sample using a feedback-controlled diode laser; the molar abundance of ^{3}He and ^{4}He/^{3}He ratio was then measured at each heating step using sector-field mass spectrometry. The ^{4}He/^{3}He release spectrum is displayed as a ratio evolution diagram where the ^{4}He/^{3}He ratio of each step (R_{step}) is normalized to the bulk ^{4}He/^{3}He ratio (R_{bulk}) of the sample, and is plotted against the cumulative released fraction of ^{3}He (ΣF_{3He}) (Shuster and Farley, 2005, 2004; Shuster et al., 2003) (Table DR2, Fig. DR3). Assuming a spatially uniform production of radiogenic ^{4}He, the data should fall within an allowable envelope between end member profiles produced by steady state production/diffusion and alpha ejection alone (Farley et al., 2010). U-Th zonation, which may skew the initial spatial distribution of ^{4}He production, or other yet unknown systematics affecting the final form of the diffusion distribution may cause ^{4}He/^{3}He data at particular steps to plot within the 'forbidden zone' outside of the end-member envelopes (Shuster and Farley, 2005, 2004). We removed such steps prior to interpreting the data and using the random search algorithm described in Schildgen et al. (2010) using RDAAM parameters (Flowers et al., 2009).

^{4}He/^{3}He Results and Modeling

ScT2's ^{4}He/^{3}He ratio evolution diagram, representing its He diffusion profile (Table DR2), overlain by model results corresponding to predicted cooling trajectories is shown in Figure DR3a. The grain analyzed for ^{4}He/^{3}He analysis, apatite grain ScT2-1_a, was a euhedral grain with no visible inclusions, had a bulk AHe age of 211 ± 5 Ma, which is within error of ScT1's average AHe age (219.2 ±17.9, Table 1). ^{4}He/^{3}He ratios increase systematically with ΣF_{3He} except for the last two steps, which encroached upon the forbidden zone and were therefore eliminated from model scoring (Shuster and Farley, 2005). We forward modeled cooling histories for ScT2's diffusion profile from 135°C to 10°C (surface temperature) for 400 Ma (~ 2x the grain age) in 1 Ma steps for 3,000 iterations allowing for 3-10 points (or bends) in the modeled t-T histories. ScT2 was the only analyzed apatite whose models produced any cooling trajectories with acceptable fits to the measured ^{4}He/^{3}He release spectrum. Acceptable fit cooling trajectories for ScT2 show a three stage cooling history: 1) cooling to ~55-40°C by ~350-250 Ma, 2) a long period of slow to stagnant cooling, and 3) renewed rapid cooling from 50-30°C to the surface beginning between 125-20 Ma (Fig. DR3a). The results of this model introduce the possibility for renewed exhumation in the Cretaceous through the Cenozoic at the Cluanie field site.

ScT1's $^{4}He/^{3}He$ ratio evolution diagram, representing its He diffusion profile (Table DR2), overlain by model results corresponding to predicted cooling trajectories is shown in Figure DR3b. The grain analyzed for $^{4}He/^{3}He$ analysis, apatite grain ScT1-3_c, was a euhedral grain with no visible inclusions, had a bulk AHe age of 111.0 ± 2.0 Ma. This grain age was not within error of ScT1's average AHe age (56.3 ±17.9, Table 1). This was our first clue that we may have difficulties interpreting the $^{4}He/^{3}He$ model results. $^{4}He/^{3}He$ ratios increase systematically with ΣF_{3He} except for steps 1, 2, and 3 were below the detection limit step 20 which encroached upon the forbidden zone and were eliminated prior to modeling (Shuster and Farley, 2005). We forward modeled cooling histories for ScT1's diffusion profile from 135°C to 10°C (surface temperature) for 200 Ma (~ 2x the grain age) in 1 Ma steps for 3,000 iterations allowing for 3-10 points (or bends) in the modeled t-T histories. Due to the large number of steps that needed to be eliminated from model scoring, the analyzed apatite's bulk AHe age that is not within error of ScT1's average AHe age, and because no cooling trajectories with an acceptable fit to the measured $^{4}He/^{3}He$ release spectrum were found, likely a result of due to unconstrained U-Th zonation in the apatite, we do not attempt to interpret this data any further.

ScT11's $^{4}He/^{3}He$ ratio evolution diagram, representing its He diffusion profile (Table DR2), overlain by model results corresponding to predicted cooling trajectories is shown in Figure DR3c. ScT11's average AHe age of 83.3 ± 20.8 Ma was used in the $^{4}He/^{3}He$ modeling (Table 1). $^{4}He/^{3}He$ ratios increase systematically with ΣF_{3He} and no steps were eliminated from the scoring of model fits. We forward modeled cooling histories for ScT11's diffusion profile from 135°C to 10°C (surface temperature) for 200

Ma (~ 2x the average age) in 1 Ma steps for 3,000 iterations allowing for 3-10 points (or bends) in the modeled t-T histories. No cooling trajectories with an acceptable fit to the measured $^4He/^3He$ release spectrum were found for sample ScT11, likely a result of due to unconstrained U-Th zonation in the apatite, we do not attempt to interpret this data any further.

ScT10's $^4He/^3He$ ratio evolution diagram, representing its He diffusion profile (Table DR2), overlain by model results corresponding to predicted cooling trajectories is shown in Figure DR3d. ScT10's average AHe age of 108.4 ± 22.3 Ma was used in the $^4He/^3He$ modeling (Table 1). $^4He/^3He$ ratios increase systematically with ΣF_{3He} until the last two steps (steps 18 and 19) where R_{step}/R_{bulk} values jump from 1.252 in step 17 to 1.582 in step 18 and 2.589 in step 19 (Table DR2). This large jump in $^4He/^3He$ ratios may indicate a ^4He rich inclusion near the grain edge. Steps 18 and 19 were therefore eliminated in the scoring of model fits. We forward modeled cooling histories for ScT10's diffusion profile from 135°C to 10°C (surface temperature) for 200 Ma (~ 2x the average age) in 1 Ma steps for 3,000 iterations allowing for 3-10 points (or bends) in the modeled t-T histories. Due to the possibility of a ^4He rich inclusion in the analyzed apatite and because no cooling trajectories with an acceptable fit to the measured $^4He/^3He$ release spectrum were found for sample ScT10, we do not attempt to interpret this data any further.

Figure DR3: $^4He/^3He$ analysis and model results are shown for samples A) ScT2 from Cluanie, and B) ScT1 from Invershiel and samples C) ScT11 and D) ScT10 from Glen Nevis. The left graph in each box is the $^4He/^3He$ release spectrum for each sample shown as a ratio evolution diagram where the $^4He/^3He$ ratio (R) of each step (R_{step}) is normalized to the total $^4He/^3He$ ratio (R_{bulk}) and is a function of the cumulative released fraction of ^3He (ΣF_{3He}). The right graph shows modeled time temperature cooling trajectories. The grey paths correspond to cooling trajectories that do not predict the bulk AHe age of the sample, and therefore they are not compared to the measured $^4He/^3He$ release spectrum. Cooling trajectories represented by green, yellow, and red paths predict the bulk AHe age of the sample. Green paths represent cooling trajectories with an acceptable fit to the measured $^4He/^3He$ release spectrum. Yellow and red paths correspond to cooling trajectories that are increasingly worse fits to the data and which can be excluded as fitting the data at a 99% confidence level (see Schildgen et al., 2010 for a more detailed discussion of modeling). The ratio evolution diagram is overlain by predicted $^4He/^3He$ release spectrums resulting from the modeled cooling trajectories. Only sample ScT2 produced any acceptable fit-paths.

Table DR2. Apatite $^4He/^3He$ data

Fig DR1

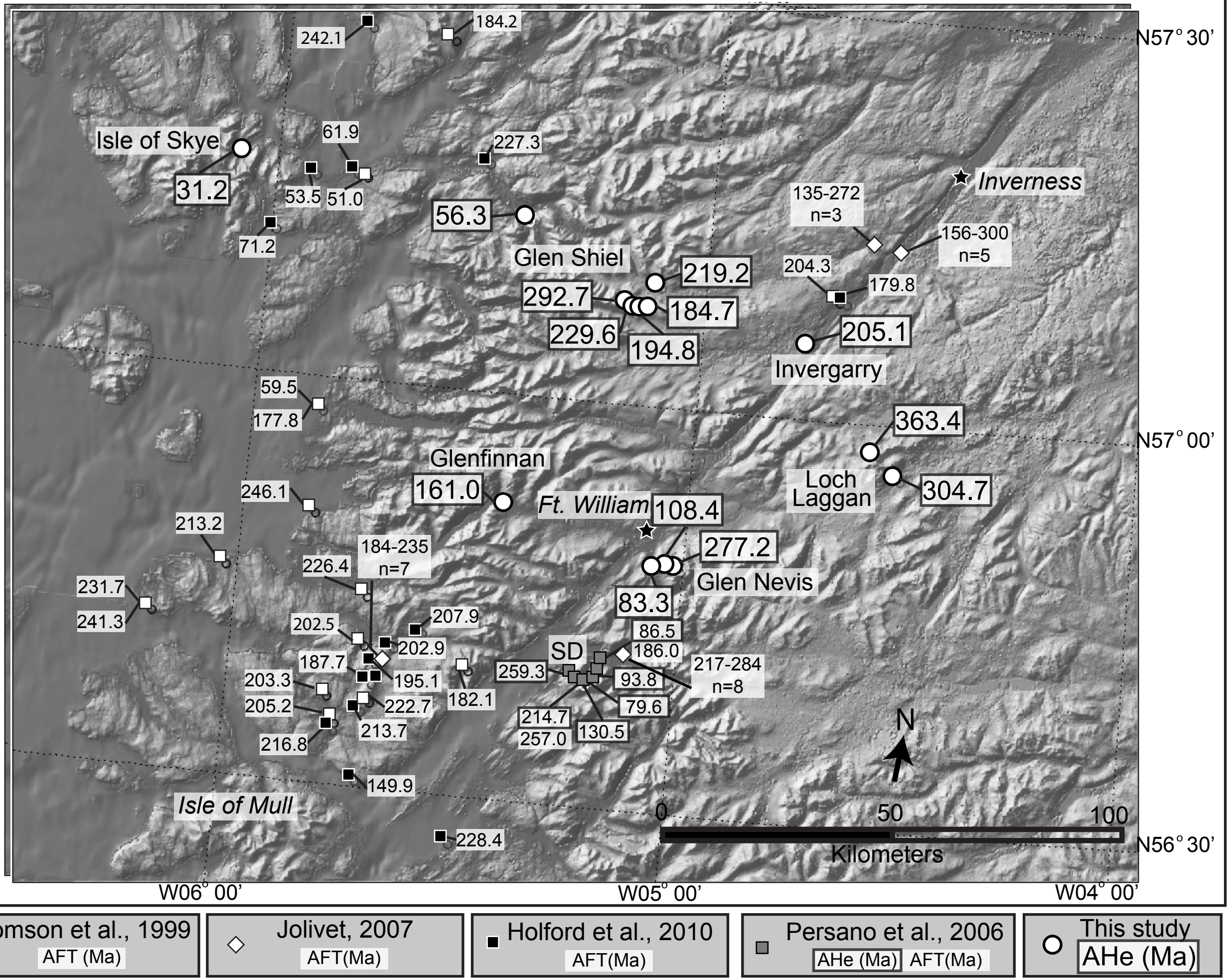

Isle of Skye
31.2
242.1
184.2
61.9
227.3
53.5
51.0
71.2
56.3
Glen Shiel
219.2
292.7
184.7
229.6
194.8
Inverness
135-272
n=3
156-300
n=5
204.3
179.8
205.1
Invergarry
59.5
177.8
363.4
Glenfinnan
161.0
Ft. William
108.4
Loch
Laggan
304.7
246.1
213.2
184-235
n=7
226.4
277.2
Glen Nevis
83.3
231.7
241.3
207.9
202.5
202.9
86.5
186.0
SD
187.7
195.1
259.3
217-284
n=8
93.8
203.3
182.1
222.7
79.6
205.2
213.7
214.7
257.0
130.5
216.8
N
149.9
Isle of Mull
0
50
100
Kilometers
228.4
N57° 30'
N57° 00'
N56° 30'
W06° 00'
W05° 00'
W04° 00'
Thomson et al., 1999
AFT (Ma)
Jolivet, 2007
AFT(Ma)
Holford et al., 2010
AFT(Ma)
Persano et al., 2006
AHe (Ma)
AFT(Ma)
This study
AHe (Ma)

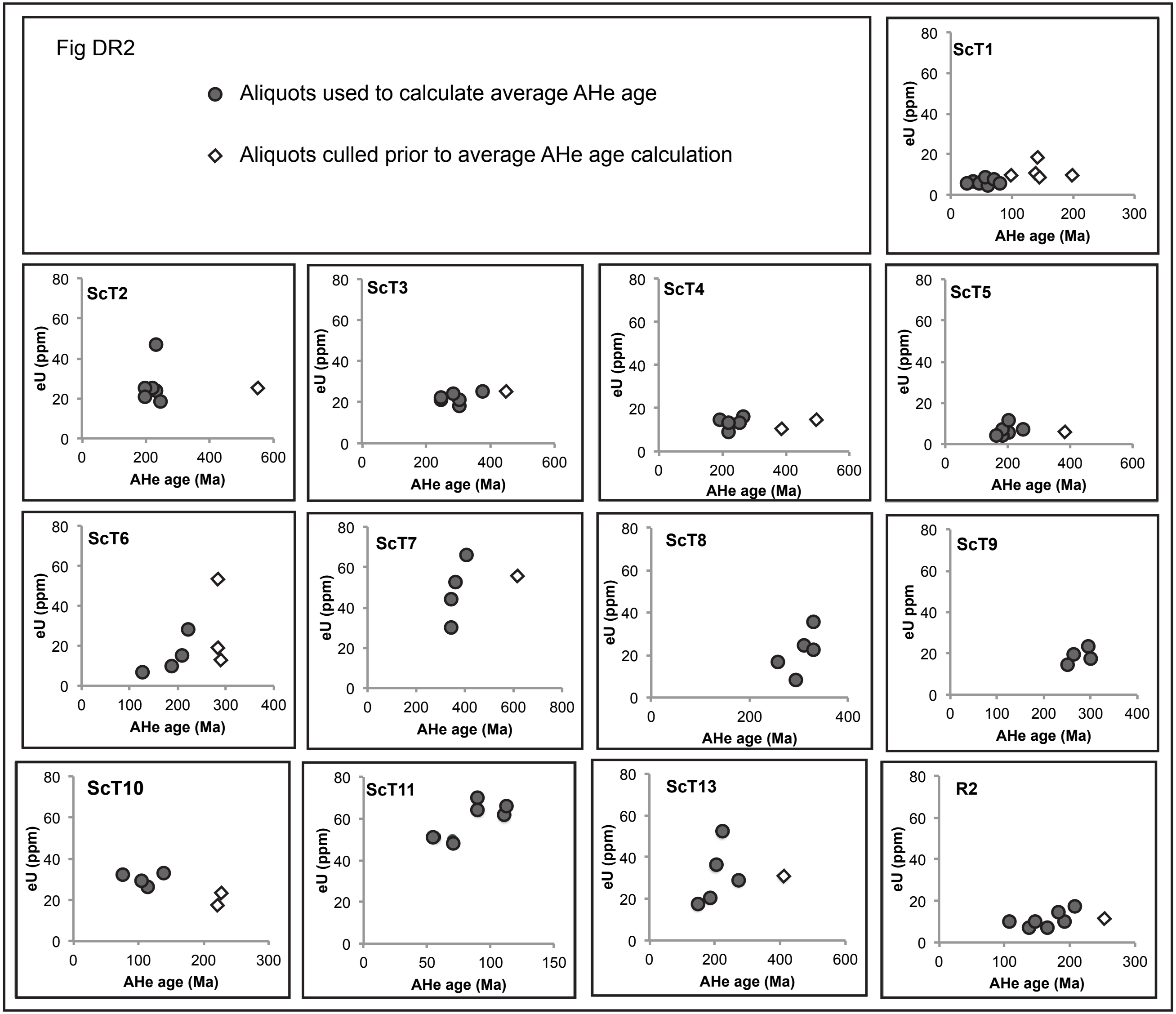
Fig DR2
Aliquots used to calculate average AHe age
Aliquots culled prior to average AHe age calculation
ScT1
ScT2
ScT3
ScT4
ScT5
ScT6
ScT7
ScT8
ScT9
ScT10
ScT11
ScT13
R2
eU (ppm)
eU ppm
AHe age (Ma)

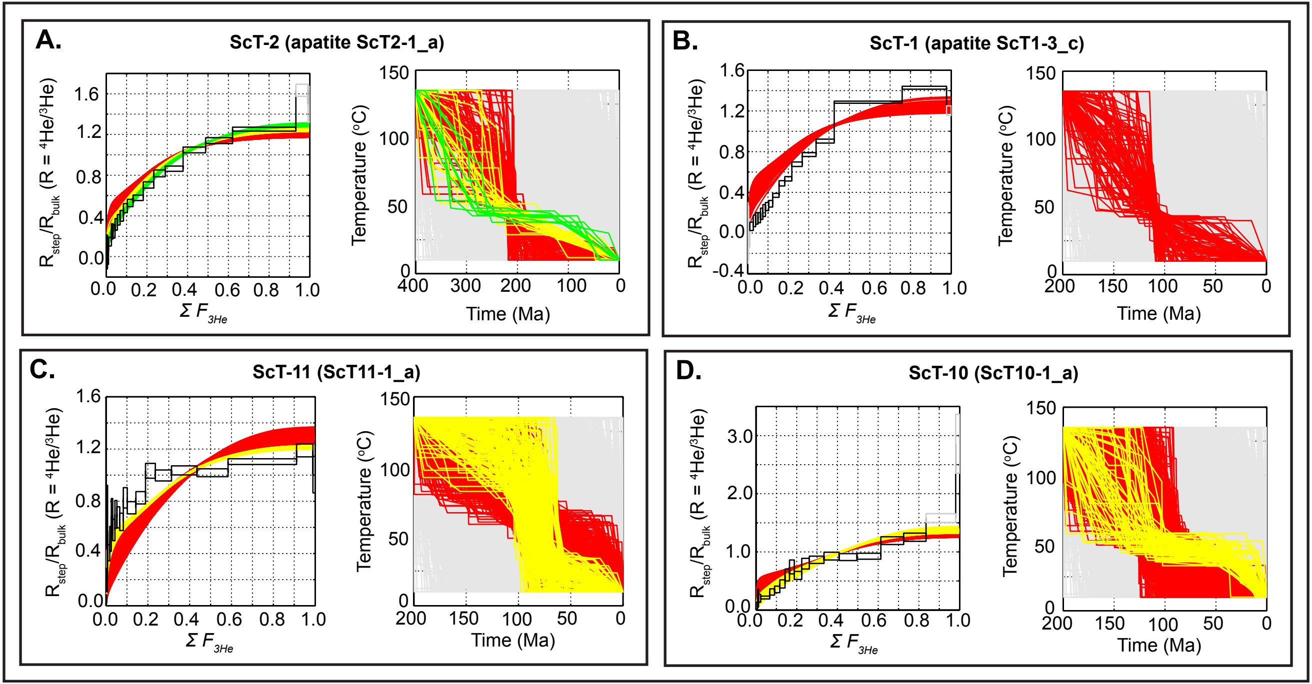
A.
ScT-2 (apatite ScT2-1_a)
B.
ScT-1 (apatite ScT1-3_c)
C.
ScT-11 (ScT11-1_a)
D.
ScT-10 (ScT10-1_a)
R_{step}/R_{bulk} ($R = {}^{4}He/{}^{3}He$)
ΣF_{3He}
Temperature (°C)
Time (Ma)
0.0
0.2
0.4
0.6
0.8
1.0
1.2
1.6
-0.4
2.0
3.0
0
50
100
150
200
300
400

Fig DR3

Fame, M.L., Spotila, J.A., Owen, L.A., Dortch, J.M., and Shuster, D.L., 2018, Spatially heterogeneous post-Caledonian burial and exhumation across the Scottish Highlands: Lithosphere, https://doi.org/10.1130/L678.1.

GSA Data Repository Item 2018139

TABLE DR1. QTQt FORWARD MODEL INPUT PARAMETERS

FM-1		FM-2		FM-3		FM-4	
t (Ma)	T (°C)	t (Ma)	T (°C)	t (Ma)	T (°C)	t (Ma)	T (°C)
0	10	0	10	0	10	0	10
15	65	55	35	70	35	90	25
55	35	60	95	90	25	110	25
60	95	66	15	110	25	130	75
66	15	70	35	130	75	140	75
70	35	90	25	140	75	200	15
90	25	110	25	200	15	225	115
110	25	130	75	225	115	245	115
130	75	140	75	245	115	350	35
140	75	200	15	350	35		
200	15	225	115				
225	115	245	115				
245	115	350	35				
350	35						
FM-1		FM-2		FM-3		FM-4	
t (Ma)	T (°C)	t (Ma)	T (°C)	t (Ma)	T (°C)	t (Ma)	T (°C)
0	10	0	10	0	10	0	10
130	75	200	15	225	115	350	35
140	75	225	115	245	115		
200	15	245	115	350	35		
225	115	350	35				
245	115						
350	35						

Note: Input time temperature points for QtQT forward thermal models (displayed in Figure 4A) based on a simplification of Holford et al. (2010) Morvern thermal history.

Fame, M.L., Spotila, J.A., Owen, L.A., Dortch, J.M., and Shuster, D.L., 2018, Spatially heterogeneous post-Caledonian burial and exhumation across the Scottish Highlands: Lithosphere, https://doi.org/10.1130/L678.1.

GSA Data Repository Item 2018139

TABLE DR2. APATITE ^{4}HE/^{3}HE DATA

Sample information	Heating step	Temperature (°C)	Step duration (hours)	(ΣF_{3He}) *	R_{step} / R_{bulk} †	R_{step}/ R_{bulk} error (±) †
Sample Name	1	210	0.20	0.003	0.051	0.164
ScT2 (apatite ScT2-1_a)	2	225	0.50	0.006	0.044	0.165
	3	260	0.38	0.011	0.055	0.131
Radial equivalence:	4	300	0.51	0.026	0.147	0.043
86.0 µm	5	300	0.66	0.034	0.248	0.075
	6	310	0.66	0.043	0.247	0.065
Apatite ScT2-1_a age	7	330	0.46	0.055	0.316	0.057
211.0 ± 5.0 Ma §	8	340	0.45	0.068	0.362	0.051
	9	350	0.48	0.085	0.401	0.052
U (ppm)	10	350	0.66	0.104	0.476	0.044
7.6	11	370	0.53	0.132	0.527	0.036
	12	400	0.48	0.182	0.578	0.027
Th (ppm)	13	410	0.50	0.234	0.704	0.031
0.1	14	420	0.56	0.290	0.818	0.033
	15	440	0.63	0.378	0.864	0.026
Model iterations	16	475	0.50	0.488	1.048	0.028
3000	17	500	0.50	0.620	1.139	0.029
	18	600	0.50	0.932	1.253	0.020
	19 #	700	0.50	0.991	1.634	0.060
	20 #	850	0.50	1.000	1.496	0.176
Sample Name	1 #	210	0.20	0.003	BDL **	0.298
ScT1 (apatite ScT1-3_c)	2 #	225	0.50	0.005	BDL **	0.268
	3 #	260	0.38	0.011	BDL **	0.137
Radial equivalence:	4	300	0.51	0.028	0.066	0.041
83.0 µm	5	300	0.66	0.040	0.119	0.056
	6	310	0.66	0.051	0.145	0.056
Apatite ScT1-3_c age	7	330	0.46	0.063	0.151	0.049
111.0 ± 2.0 Ma §	8	340	0.45	0.075	0.189	0.055
	9	350	0.48	0.088	0.221	0.058
U (ppm)	10	350	0.66	0.103	0.260	0.040
11.1	11	370	0.53	0.123	0.288	0.032
	12	400	0.48	0.155	0.370	0.019
Th (ppm)	13	410	0.50	0.183	0.489	0.026
0.1	14	420	0.56	0.217	0.534	0.022
	15	435	0.50	0.268	0.676	0.022
Model iterations	16	475	0.50	0.336	0.772	0.019
3000	17	500	0.50	0.425	0.904	0.019
	18	600	0.50	0.759	1.286	0.010
	19	700	0.50	0.977	1.428	0.015
	20 #	850	0.50	1.000	1.203	0.047
Sample Name	1	210	0.20	0.003	0.052	0.033
ScT11 (apatite ScT11_a)	2	225	0.50	0.006	0.197	0.091
	3	260	0.38	0.008	0.573	0.349
Radial equivalence:	4	300	0.51	0.018	0.405	0.061
69.8 µm	5	300	0.66	0.025	0.512	0.096
	6	310	0.66	0.032	0.687	0.134
Average age	7	330	0.46	0.043	0580	0.082
83.3 ± 20.8 Ma	8	340	0.45	0.052	0.700	0.106
	9	350	0.48	0.066	0.677	0.081
U (ppm)	10	350	0.66	0.083	0.642	0.066
38.6	11	370	0.53	0.102	0.826	0.078
	12	400	0.48	0.143	0.750	0.046
Th (ppm)	13	410	0.50	0.189	0.827	0.047
80.6	14	420	0.56	0.236	1.033	0.057
	15	440	0.63	0.313	0.997	0.042
Model iterations	16	475	0.50	0.435	1.036	0.035
3000	17	500	0.50	0.584	1.018	0.030
	18	600	0.50	0.911	1.103	0.022
	19	700	0.50	0.989	1.189	0.049
	20	850	0.50	1.000	1.004	0.140
Sample Name	1	210	0.20	0.008	0.077	0.058
ScT10 (apatite ScT10_a)	2	225	0.50	0.012	0.207	0.156
	3	260	0.38	0.023	0.202	0.067
Radial equivalence:	4	300	0.51	0.068	0.215	0.024
50.0 µm	5	300	0.66	0.091	0.311	0.054
	6	310	0.66	0.117	0.355	0.056
	7	330	0.46	0.143	0.449	0.070
Average age	8	340	0.45	0.165	0.603	0.103
108.4 ± 22.3 Ma	9	350	0.48	0.188	0.742	0.119
	10	350	0.66	0.225	0.595	0.069
U (ppm)	11	370	0.53	0.262	0.798	0.092
15.5	12	400	0.48	0.334	0.864	0.063
	13	410	0.50	0.408	0.927	0.067
Th (ppm)	14	420	0.56	0.496	0.911	0.059
46.8	15	440	0.63	0.613	0.926	0.051
	16	475	0.50	0.725	1.193	0.067

Model iterations	17	500	0.50	0.835	1.252	0.070
3000	18 #	600	0.50	0.981	1.582	0.075
	19 #	700	0.50	1.000	2.859	0.507

* Cumulative released fraction of ^3He

† R_{step} is the $^4He/^3He$ ratio of each step and is normalized to R_{bulk}, the total $^4He/^3He$ ratio.

§ Due to low analytical error on bulk grain age we input 2x error in model runs to allow more t-T paths to be compared to release spectrum

# Indicates step was removed from the model scoring.

** Below Detection Limit